Daily, seasonal, and intraseasonal relationships between lightning and NO_2 over the Maritime Continent

(Supplementary material)

Katrina S. Virts[1], Joel A. Thornton[1], John M. Wallace[1], Michael L. Hutchins[2], Robert H. Holzworth[2], and Abram R. Jacobson[2]

[1]Department of Atmospheric Sciences, University of Washington, Seattle, WA

[2]Department of Earth and Space Sciences, University of Washington, Seattle, WA

1. Statistical significance of correlations

We elected to analyze GOME-2 NO_2 retrievals rather than SCIAMACHY retrievals in hopes that the larger sample size provided by GOME-2's larger footptint would more than compensate for the larger r.m.s. error of the GOME-2 retrievals. Using 3.5 years of daily GOME-2 observations in 1281 1° × 1° grid boxes extending over the domain of the analysis provides over 10^6 observations. Based on the Student's *t* test, we ascertained that the 99% significance level for composite correlation coefficients between daily NO_2 concentrations and lightning flashes in 1° × 1° grid boxes that were used to construct the regression maps in Fig. 2 is 0.02. This significance level was obtained by making the conservative assumption that, of the 100 reference grid boxes used in the analysis, 50 are independent. Assuming that all 100 are independent implies that correlation coefficients of 0.01 are significant at the 99% level. The observed composite correlations are on the order of 0.05 to 0.07. The high level of significance of the correlations is evidenced by the smoothness of the patterns.

2. Further specifics on the performance of WWLLN

WWLLN's stroke detection efficiency has been compared in detail to simultaneous observations by the far more sensitive Los Alamos Sferic Array [*Smith et al.*, 2002]. The WWLLN detection efficiency was found in this manner to depend primarily on stroke current amplitude, and not directly on stroke type [*Jacobson et al.*, 2006]. Thus, although not a "total lightning" detection system, WWLLN is biased toward high current alone, and has no overt selection for ground strokes over cloud strokes. To that extent, WWLLN might be expected to serve as a reasonable interim proxy for lightning NO_x production, at least for the period before total-lightning monitors are operational. WWLLN data do not contain any indication of stroke altitude.

The median global very low frequency (VLF) stroke power measured by WWLLN is 3×10^6 W, more than three orders of magnitude smaller than that indicated by previous measurements, which have shown the power radiated by strokes to be near 10^{10} W [*Krider and Guo*, 1983]. However, this apparent discrepancy is due to the difference in methodology. Previous measurements were of broad band peak power taken in the near field (within 100 km of the lightning stroke), whereas WWLLN measures the r.m.s. power in the 6-18 kHz band in the far field. With these factors accounted for, the median power is comparable to the previously reported value of 10^{10} W [*Krider and Guo*, 1983].

3. Sensitivity tests on daily lightning/NO_2 relationship and NO_2/stroke estimate

Figure 2 in *Virts et al.* [2011] shows the results of a composite lag regression analysis of daily lightning frequency and tropospheric NO_2 column density fields over Indonesia (see text for details). To test the robustness of these results, we have conducted a series of sensitivity studies, varying the following aspects of the analysis (note that for each estimate of NO_2 production, a WWLLN detection efficiency of 10% was assumed).

- **Cloud fraction threshold** The results shown in *Virts et al.* [2011] were obtained by analyzing only tropospheric NO_2 retrievals classified as "meaningful" by the GOME-2 research team's algorithms [*Boersma et al.*, 2004]. To test the impact of cloudy observations, the composite lag regression analyses were repeated with NO_2 time series that incorporated only observations for which the FRESCO cloud fraction [*Koelemeijer et al.*, 2011] was below 0.1 (Fig. S1).

- **Sample size** Although it is clearly desirable to choose reference boxes for which there is sufficient lightning to provide a day-to-day signal, our selection of the 100 grid boxes with the highest annual-mean lightning frequencies is somewhat arbitrary. Lag regression analyses performed using reference boxes with lightning frequencies in the top 50 and 500 are shown in Fig. S2.
- **Location of reference boxes** To test whether our results are sensitive to possible changes in the NO_2 plume from surface sources along the Indonesian islands, the lag regression analysis was repeated using a set of reference boxes located over water or over less polluted land areas (Fig. S3). The associated composite NO_2 regression patterns are shown in Fig. S4.

Comparison of Figs. S1, S2, and S4 and Fig. 2 in the text shows that the spatial pattern and temporal evolution of the NO_2 field are robust with respect to variations in the analysis protocol. The production efficiencies estimated on the basis of these various protocols were used to obtain the estimated range of 1 to 2×10^{25} NO_2 molecules per stroke put forth in *Virts et al.* [2011].

4. MJO correlation maps

Figure S5 shows maps of correlations between the MJO index and clouds, lightning, and NO_2, analogous to Fig. 4 in the text. It is evident that the MJO signal in lightning and NO_2 over the eastern Indian Ocean is strongest just to the west of Sumatra, within the region in which mesoscale circulations driven by land/sea contrasts and terrain play an important role in triggering convection.

5. Alternative explanations for NO_2 patterns

In this section we examine three factors that can influence tropospheric NO_2 column retrievals and discuss whether they could produce the NO_2 patterns shown in *Virts et al.* [2011].

- **Tropopause height variations**. Tropospheric NO_2 vertical column densities are obtained from total atmospheric slant column densities by subtracting an assumed stratospheric NO_2 column and dividing by a tropospheric air mass factor [*Boersma et al.*, 2004]. The MJO modulates cold-point tropopause height; however, these variations are on the planetary scale [e.g., *Zhang*, 2005; *Virts and Wallace*, 2010] and thus cannot explain the more localized NO_2 patterns in Figs. 4 and S5.
- **Transport of non-lightning NO_2**. NO_2 produced by surface sources can be transported by convection to the upper troposphere, where its lifetime is longer and where it is more readily visible to the satellite. Winds can also transport NO_2 horizontally, as seen in Fig. 2 in the text. We have demonstrated that the plume of enhanced NO_2 associated with a lightning maximum is present regardless of whether we use reference boxes over the ocean or over less polluted land areas (Fig. S4). In addition, the MJO NO_2 signature in Figs. 4 and S5 is strongest to the west of Sumatra, where the influence of surface sources of NO_2 is much lower (e.g., Fig. 1).
- **Cloud contamination**. The dissimilarities in the cloud and NO_2 patterns in Figs. 1 and 4, combined with the fact that the NO_2 patterns in Figs. 2 and 4 do not change when only NO_2 retrievals with cloud fractions below 0.1 are included in the analysis (see, e.g., Fig. S1), indicate that cloud contamination is not a significant issue for these analyses, though it may be important for absolute quantification of the lightning NO_x source.

Thus, while each of these factors influences GOME-2's tropospheric NO_2 retrievals, none can account for the NO_2 patterns associated with lightning shown in the text. Other factors that impact tropospheric NO_2 retrievals are discussed in *Boersma et al.* [2004].

References

Beirle, S., H. Huntrieser, and T. Wagner (2010), Direct satellite observation of lightning-produced NO_x, *Atmos. Chem. Phys.*, *10*, 10965-10986.

Boersma, K. F., H. J. Eskes, and E. J. Brinksma (2004), Error analysis for tropospheric NO_2 retrieval from space, *J. Geophys. Res.*, *109*, D04311, doi:10.1029/2003JD003962.

Jacobson, A. R., R. H. Holzworth, J. Harlin, R. L. Dowden, and E. H. Lay (2006), Performance assessment of the World Wide Lightning Location Network (WWLLN), using the Los Alamos Sferic Array (LASA) as ground-truth, *J. Atmos. Ocean. Tech.*, *23*, 1082-1092.

Koelemeijer, R. B. A., P. Stammes, J. W. Hovenier, and J. F. de Haan (2001), A fast method for retrieval of cloud parameters using oxygen A band measurements from the Global Ozone Monitoring Experiment, *J. Geophys. Res.*, *106*, 3475-3490.

Krider, E. P., and C. Guo (1983), The peak electromagnetic power radiated by lightning return strokes, *J. Geophys. Res.*, *88(C13)*, 8471-8474, doi:10.1029/JC088iC13p08471.

Smith, D. A., K. B. Eack, J. Harlin, M. J. Heavner, A. R. Jacobson, R. S. Massey, X. M. Shao, and K. C. Wiens (2002), The Los Alamos Sferic Array: A research tool for lightning investigations, *J. Geophys. Res.*, *107(D13)*, doi:10.1029/2001JD000502.

Virts, K. S., J. A. Thornton, J. M. Wallace, M. L. Hutchins, R. H. Holzworth, and A. R. Jacobson (2011), Daily, seasonal, and intraseasonal relationships between lightning and NO_2 over the Maritime Continent, *Geophys. Res. Lett.*, ???.

Virts, K. S., and J. M. Wallace (2010), Annual, interannual, and intraseasonal variability of tropical tropopause transition layer cirrus, *J. Atmos. Sci.*, *67*, 3097-3112.

Zhang, C., (2005), Madden-Julian Oscillation, *Rev. of Geophys.*, *43*, RG2003, doi:10.1029/2004RG000158.

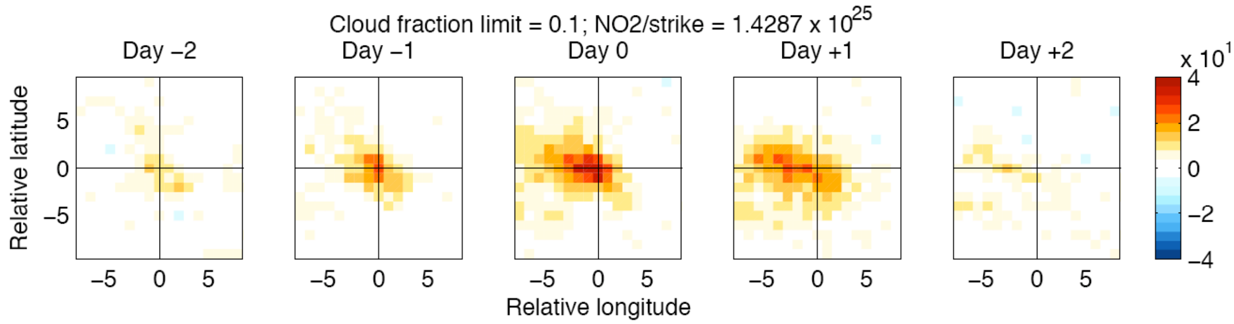

Figure S1. As in Fig. 2, but NO_2 time series were calculated using only observations with FRESCO cloud fractions less than 0.1.

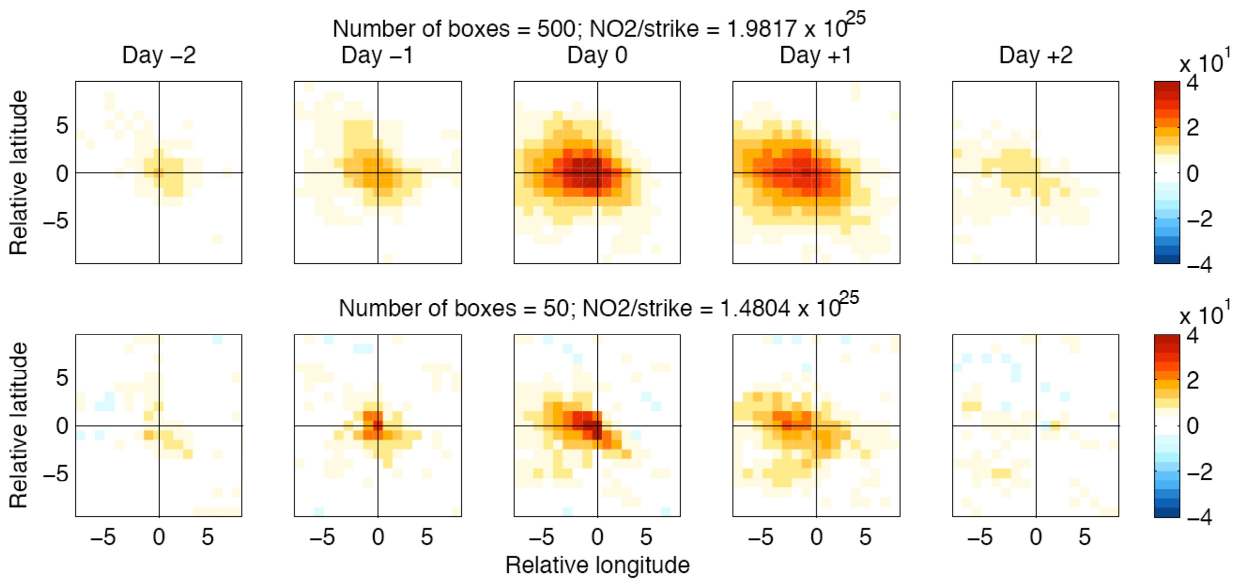

Figure S2. As in Fig. 2, but regressions were calculated using the indicated number of reference boxes.

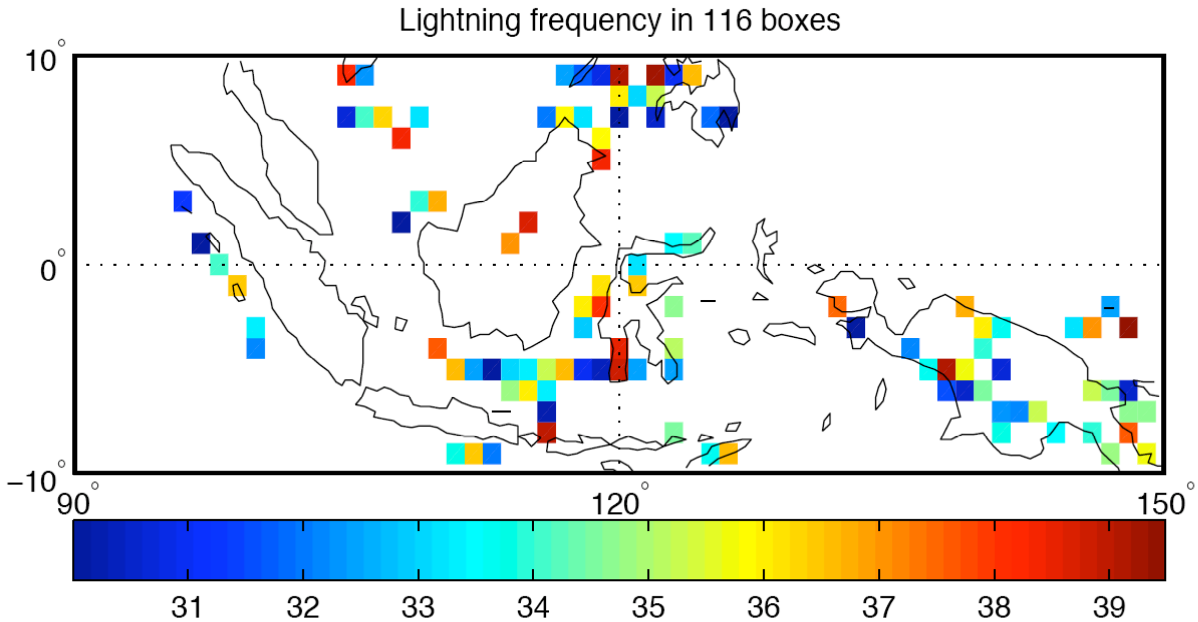

Figure S3. Annual-mean lightning frequency in selected grid boxes over water or less polluted land areas.

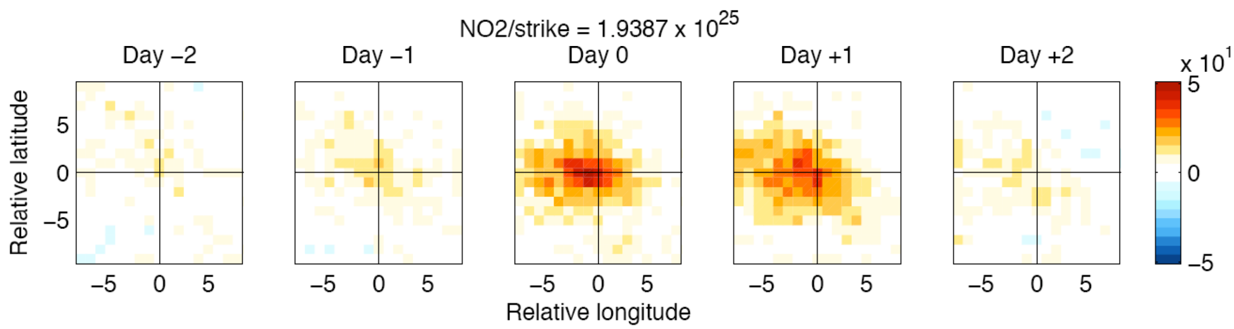

Figure S4. As in Fig. 2, but regressions were calculated using the reference boxes shown in Fig. S3.

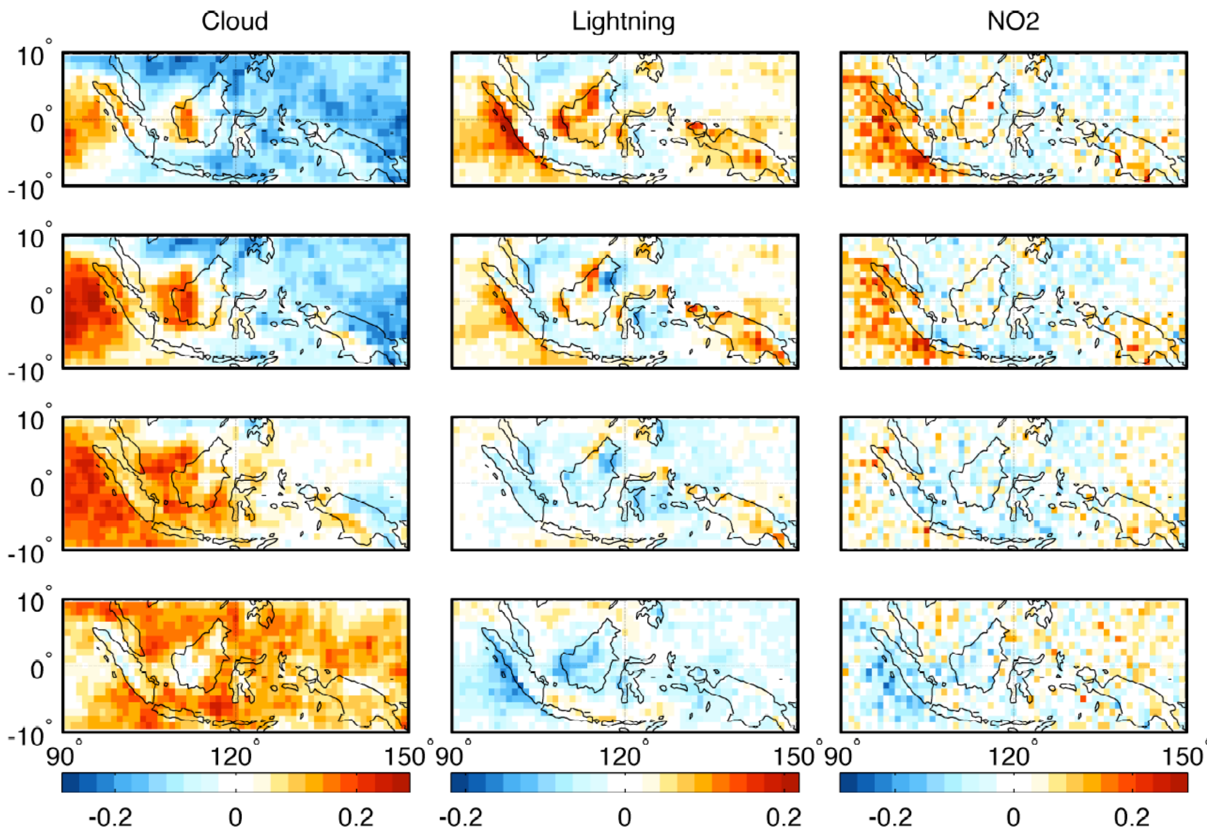

137 **Figure S5.** As in Fig. 4, but cloud, lightning, and NO_2 are correlated with MJO indices.